Design and simulation of a novel CMOS superimposed photodetector*

KANG Yu-zhuo(康玉琢)**, **MAO Lu-hong**(毛陆虹), **XIAO Xin-dong**(肖新东), **XIE Sheng**(谢生), **and ZHANG Shi-lin**(张世林)

School of Electronic Information Engineering, Tianjin University, Tianjin 300072, China

(Received 19 March 2012)

A novel superimposed photodetector (PD) is put forward. The photodetector can obtain a couple of differential photocurrent signals from one input optical signal. The light injection efficiency and the vertical work distance of this new photodetector are much higher than those of the others. The superimposed photodetctor is designed based on the standard 0.18 μm CMOS process. The responsivity, bandwidth and transient response of the photodetector are simulated by a commercial simulation software of ATLAS. The responsivities of two obtained photocurrent signals are 0.035 A/W and 0.034 A/W, while the bandwidths are 3.8 GHz and 5.2 GHz, respectively. A full differential optical receiver which uses the superimposed photodetector as input is simulated. The frequency response and 4 Gbit/s eye diagram of the optical receiver are also obtained. The results show that the two output signals can be used as the differential signal.

Document code: A **Article ID:** 1673-1905(2012)04-0249-4

DOI 10.1007/s11801-012-1150-z

In many communication systems, data transmission speed has been the bottleneck of system performance[1]. But optical communication technology can solve this issue effectively, so the photodetector (PD) and the optical receiver have been researched in recent years[2-4].

For the low cost of standard CMOS process, the research of the optical receivers which are integrated with CMOS compatible PD grows fast in recent years[5-7]. But because of the low absorption coefficient of silicon, designing high speed PDs on Si is much more difficult than other very expensive processes like on GaAs[8,9] and InGaAs[10,11]. It reduces the performance of CMOS compatible optical receiver seriously. The metal-semiconductor-metal photodetector (MSM-PD) implemented on thin polycrystalline silicon layer[12] and the P-N junction PD fabricated in well[13] which is named double-photodetector (DPD) can achieve high speed, but their vertical work distances are limited by the thickness of polycrystalline silicon layer and the well depth, which means their responsivities are low.

A well designed circuit structure can enhance the performance of optical receiver effectively. Differential structure is always used in high performance applications for its high stability, high sensitivity and low noise. The problem of full differential optical receiver is that it needs a pair of differential input signals, which makes the system complex.

To solve these issues, the concept of superimposed PD is proposed in this paper. This kind of photodetector can increase the vertical work distance of PD, improve the absorption coefficient, and obtain two photocurrent signals under one incident optical signal.

Structure of the superimposed PD is shown in Fig.1. MSM-PD is implemented on polycrystalline silicon (POLY1), and DPD is implemented on P type substrate (P_{SUB}). There are two layers of SiO_2 between the MSM-PD and the DPD to prevent photogenic carrier generated from one of them diffusing to another. The heavy doping polycrystalline silicon (POLY2) between the two SiO_2 layers should be bonded to ground to separate the electrical fields in two PDs. Then the electrical field in any one of the PDs can not change the depletion region in the other one.

The $P+/N_{WELL}$ junction acts as the work diode of DPD. Considering the most photocurrent of DPD is generated in N_{WELL}, increasing the depth of N_{WELL} results in the responsivity improved. Increasing the reverse bias voltage is another way to enhance responsivity, but it is not very effective. The direct current (DC) response of DPD to reverse bias voltage at

* This work has been supported by the National Natural Science Foundation of China (No. 61036002), and the Natural Science Foundation of Tianjin (No.11JCZDJC15100).

** E-mail: kfsx@hotmail.com

different N_{WELL} depths is shown in Fig.2(a). It is simulated by ATLAS. As can be seen, the depth of N_{WELL} dominates the increase of photocurrent.

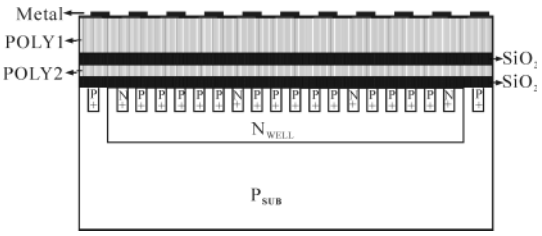

Fig.1 Schematic diagram of the device structure

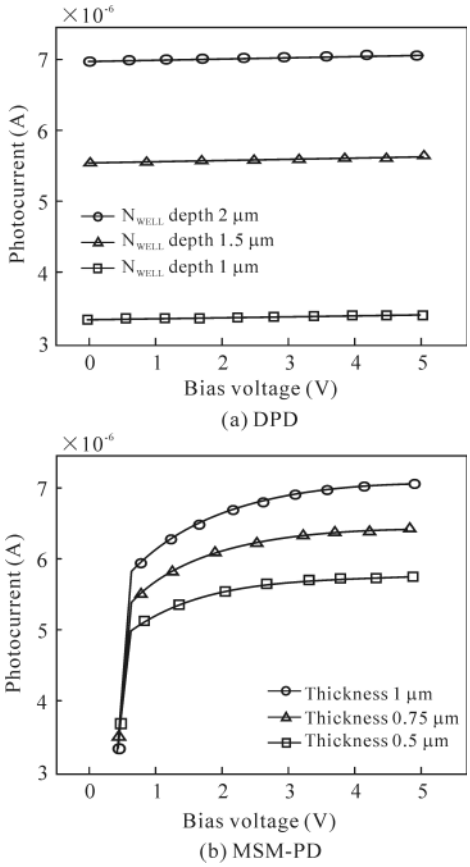

Fig.2 DC response to reverse bias voltage of DPD and MSM-PD at different N_{well} depths and device thicknesses

In this paper, MSM-PD is implemented on the polycrystalline silicon (POLY1). The photocurrent completely consists of the photogenic charge carriers in polycrystalline silicon. So, under a fixed doping concentration, the thickness of polycrystalline silicon is a main factor for MSM-PD's responsivity. Bias voltage is another important factor. When the bias voltage of MSM-PD is lower than flat band voltage (V_{FB}), the increase of bias voltage makes the photocurrent increase quickly. When the bias voltage of MSM-PD is higher than V_{FB}, the photocurrent keeps static in substance[14]. The V_{FB} is given by[15]:

$$V_{FB}=qNL^2/2\varepsilon_r\varepsilon_0 , \tag{1}$$

where N is doping concentration, L is electrode spacing, ε is the permittivity of silicon, and q is the elementary charge. DC photocurrent response of MSM-PD to reverse bias voltage under different device thicknesses is shown in Fig.2(b).

The bandwidth of PD depends on RC time constant of device and transit time of carries. Capacitance of DPD equals the reverse capacitance of PN junction with the same junction area. It can be calculated by $C_T=A\varepsilon_r\varepsilon_0/W$, where A is PN junction area, ε is permittivity of silicon, and W is depletion region width. The capacitance of DPD with the area of 50 μm × 50 μm, the N_{WELL} doping concentration of 1×10^{17} cm^{-2} and the P + doping concentration of 1×10^{20} cm^{-2} is about 1 pF.

The photogenic charge carriers of DPD consist of drifting carriers and diffusing carriers. The count and moving distance of diffusing carriers influence the bandwidth of DPD seriously, which means the depth of N_{WELL} determines the bandwidth of DPD. This effect is represented in Fig.3.

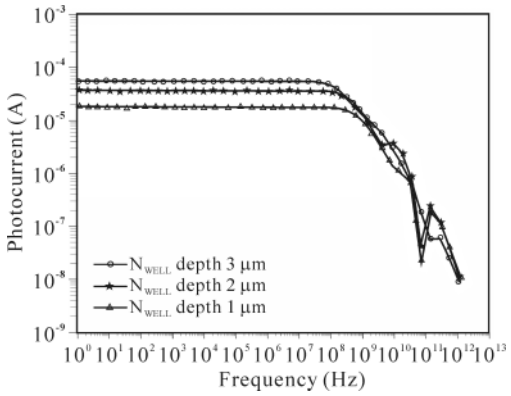

Fig.3 Simulation of DC response to frequency for DPDs with different N_{WELL} depths

The capacitance of MSM-PD equals the capacitance of its planar interdigitated metal electrodes, which can be calculated by[12]

$$C_{MSM}=L(n-1)\varepsilon_r\varepsilon_0K(k)/K(k') , \tag{2}$$

where ε is the permittivity of silicon, L is the finger length, and n is the number of fingers. $K(k)$ is the complete elliptic integral of the first kind, which can be written as

$$K(k)=\int_0^{\pi/2}\frac{1}{\sqrt{1-k^2\sin^2\varphi}}\mathrm{d}\varphi , \tag{3}$$

$$k=\tan^2\left[\frac{\pi w}{4(d+w)}\right],\quad k'=\sqrt{1-k^2} , \tag{4}$$

where w is the finger width, and d is finger spacing. When w and d are both 1 μm, the capacitance of MSM-PD with an area of 50 μm × 50 μm is 0.06 pF.

The electric field between adjacent electrodes is reduced with the depth of the device increasing, which results in the velocity of carrier decreasing. So the bandwidth of MSM-PD is decreased by increasing the device thickness, which is shown in Fig.4.

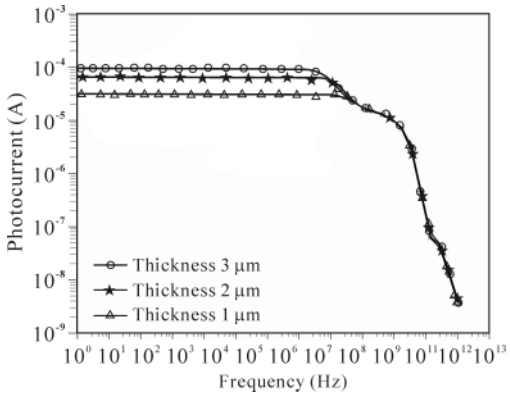

Fig.4 Simulation of DC response to frequency for MSM-PD with different device thicknesses

The DPD is composed of P_{SUB}, N_{WELL}, N+ and P+. The doping concentration of P_{SUB} is 1×10^{16} cm^{-3}. The depth and doping concentration of N_{WELL} are 1.75 μm and 1×10^{17} cm^{-3}, respectively. The junction depth and doping concentration of N+ and P+ are 0.16 μm and 1×10^{20} cm^{-3}, respectively. The MSM-PD is composed of POLY1 and the interdigitated electrodes on its surface. The thickness of POLY1 is 1 μm. The width and spacing of electrodes are both 0.5 μm. DPD and MSM-PD are separated by two layers of SiO_2 and POLY2. POLY2 is heavily doped and bonded to ground. The PD area is 50 μm×50 μm. The simulation is under the incident light power of 1 mW. The photocurrent, capacitance and width of DPD are 35.79 μA, 1.1 pF and 3.8 Gbit/s, respectively. The photocurrent of MDM-PD is 34.73 A, while the capacitance is 0.08 pF, and the bit rate is 5.2 Gbit/s. Fig.5 shows the frequency response and transient response of photocurrent for the superimposed PD.

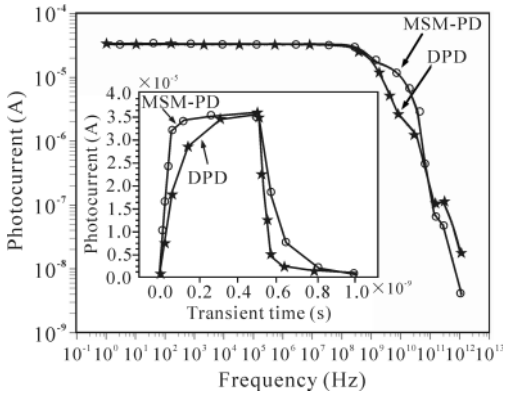

Fig.5 Frequency response and transient response (inset) of photocurrent for the simulated superimposed photodetector

The Cadence model of the superimposed PD is built based on the simulating results above. This model is used as the input PD of a full differential optical receiver based on Chartered 0.18 μm CMOS process. Fig.6 is the simulated frequency response of gain for the optical receiver, and the bandwidth is 3.61 GHz. Fig.7 shows the simulated eye diagram under a 4 Gbit/s input signal.

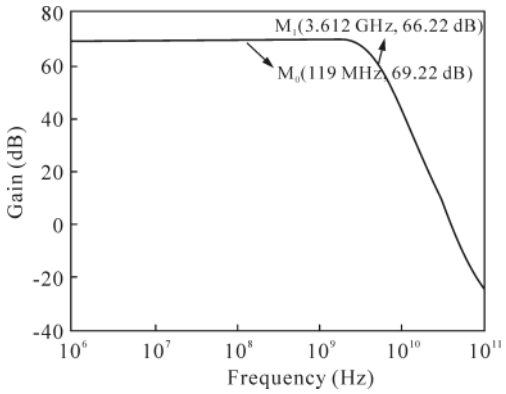

Fig.6 Frequency response simulation of gain for a full differential optical receiver

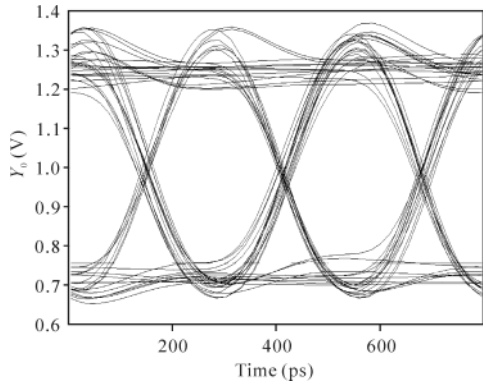

Fig.7 Simulated eye diagram under 4 Gbit/s pseudo-random input signal

In this paper, a superimposed PD is proposed. This PD can obtain two photocurrent signals from one incident optical signal, and can increase the light injection efficiency. Referring to the 0.18 μm CMOS process, the corresponding photodetector with the area of 50 μm × 50 μm is designed and simulated. A differential optical receiver with this PD based on the same process is also simulated. Results show that the outputs of the PD can be used as a couple of differential inputs for a differential optical receiver.

References

[1] Filip Tavernier and Michel S. J. Steyaert, Solid-State Circuits **44**, 2856 (2009).

[2] Stewart D. Personick, Journal of Lightwave Technology **26**, 1005 (2008).

[3] ZHOU Zhi-wen, HE Jing-kai, WANG Rui-chun, LI Cheng and YU Jin-zhong, Journal of Optoelectronics • Laser **21**, 59 (2010). (in Chinese)

[4] Kao T. S.-C and Carusone A. C, A 5-Gbps Optical Receiver with Monolithically Integrated Photodetector in 0.18 μm CMOS, IEEE Radio Frequency Integrated Circuits Symposium (RFIC), 451 (2009).

[5] Mausumi Maitra, Kaushik Chakraborty and Shubhajit Roy Chowdhury, A Comparative Study on ASIC Design of High Frequency Low Power Photoreceiver Using 0.15 μm CMOS Technology, International Conference on Electrical and Computer Engineering (ICECE), 101 (2010).

[6] Filip Tavernier and Michiel Steyaert, Power Efficient 4.5 Gbit/s Optical Receiver in 130 nm CMOS with Integrated Photodiode, 34 th European Solid-State Circuits Conference, 162 (2008).

[7] XIAO Xin-dong, MAO Lu-hong, YU Chang-liang, ZHANG Shi-lin and XIE Sheng, Journal of Optoelectronics • Laser **21**, 520 (2010). (in Chinese)

[8] M. Mikulics, S. Wu, M. Marso, R. Adam, A. Forster, A. van der Hart, P. Kordos, H. Luth and R. Sobolewski, Photonics Technology Letters **18**, 820 (2006).

[9] Linus C. Chuang, Chris Chase, Michael Moewe, Kar Wei Ng, Shanna Crankshaw and Connie Chang-Hasnain, GaAs Nanoneedle Photodetector Monolithically Grown on a (111) Si Substrate by MOCVD, Conference on Lasers and Electro-Optics and Quantum Electronics and Laser Science (CLEO/QELS), 1 (2009).

[10] Y. S. Wang, S. J. Chang, C. L. Tsai, M. C. Wu, Y. Z. Chiou, Y. H. Huang and W. Lin, IEEE Transactions on Electron Devices **56**, 1347 (2009).

[11] O. Parillaud, O. Huet, J. Decobert, M. Garrigues, R. Gil-Sobraques and J.-L. Leclercq, Realization of a Tunable Near Infrared InP / InGaAs QWs based Photodetector Integrated in a MOEMS Structure for Micro-Spectrometer Applications, IEEE International Conference on Indium Phosphide & Related Materials (IPRM), 285 (2009).

[12] Elena Budianu, Munizer Purica, Elena Manea, Mihai Danila, Raluca Gavrila and Isabella Oprea, Design and Optimization of an MSM Photodetector based on Poly-Si Layer, Proceedings of International Semiconductor Conference, 181 (2001).

[13] T. K. Woodward and Ashok V. Krishnamoorthy, Quantum Electronics **5**, 146 (1999).

[14] WU Shu, LIN Shi-ming and LIU Wen-kai, Journal of Optoelectronics • Laser **12**, 552 (2001). (in Chinese)

[15] S. M. SZE, D. J. Coleman Jr. and A. Loya, Solid-State Electronics **14**, 1209 (1971).